Geophysical Research Letters

RESEARCH LETTER
10.1029/2018GL079698

Key Points:
- Models with higher global hydrologic sensitivity project larger extreme precipitation increases in tropical and some extratropical regions
- Models with a larger increase in extreme precipitation exhibit compensating larger declines or smaller increases in light-moderate events
- The results showcase links between hydrologic cycle projections across spatial scales and offer new perspectives for constraining extremes

Supporting Information:
- Supporting Information S1

Correspondence to:
C. W. Thackeray,
cwthackeray@ucla.edu

Citation:
Thackeray, C. W., DeAngelis, A. M., Hall, A., Swain, D. L., & Qu, X. (2018). On the connection between global hydrologic sensitivity and regional wet extremes. *Geophysical Research Letters*, *45*. https://doi.org/10.1029/2018GL079698

Received 19 JUL 2018
Accepted 5 OCT 2018
Accepted article online 10 OCT 2018

On the Connection Between Global Hydrologic Sensitivity and Regional Wet Extremes

Chad W. Thackeray[1], Anthony M. DeAngelis[1,2,3], Alex Hall[1], Daniel L. Swain[4,5], and Xin Qu[1]

[1]Department of Atmospheric and Oceanic Sciences, University of California, Los Angeles, CA, USA, [2]Now at Global Modeling and Assimilation Office, NASA Goddard Space Flight Center, Greenbelt, MD, USA, [3]Science Systems and Applications, Inc., Lanham, MD, USA, [4]Institute of the Environment and Sustainability, University of California, Los Angeles, CA, USA, [5]The Nature Conservancy, Arlington, VA, USA

Abstract A highly uncertain aspect of anthropogenic climate change is the rate at which the global hydrologic cycle intensifies. The future change in global-mean precipitation per degree warming, or hydrologic sensitivity, exhibits a threefold spread (1–3%/K) in current global climate models. In this study, we find that the intermodel spread in this value is associated with a significant portion of variability in future projections of extreme precipitation in the tropics, extending also into subtropical atmospheric river corridors. Additionally, there is a very tight intermodel relationship between changes in extreme and nonextreme precipitation, whereby models compensate for increasing extreme precipitation events by decreasing weak-moderate events. Another factor linked to changes in precipitation extremes is model resolution, with higher resolution models showing a larger increase in heavy extremes. These results highlight ways various aspects of hydrologic cycle intensification are linked in models and shed new light on the task of constraining precipitation extremes.

Plain Language Summary The global water cycle is expected to intensify under climate change and can be generally characterized by greater rainfall and surface evaporation in the future. However, the rate at which the globally averaged precipitation increases is highly variable among different climate models. In this paper, we relate the intermodel variability in global water cycle intensification to differences in model projections of heavy precipitation in tropical and some extratropical regions. We also find that models consistently experience a trade-off between increasing heavy and decreasing light-moderate precipitation: Models with larger future increases in heavy precipitation exhibit greater compensating declines in light-moderate rainfall. Differences in heavy precipitation changes are also tied to model resolution. Our study helps to provide new insight on the factors shaping projections of future precipitation extremes, which have strong implications for water resources, natural hazard risks associated with flooding, and ecosystem stability.

1. Introduction

As the climate warms, various components of the global atmospheric energy budget (i.e., longwave cooling, shortwave heating, and surface sensible heat flux) must change in response. Because the atmosphere cannot store energy on long time scales, an adjustment in the form of latent heat release (evaporation and precipitation) occurs to balance radiative and sensible heat changes (DeAngelis et al., 2015, 2016; Pendergrass & Hartmann, 2014a). Additionally, atmospheric water vapor increases rapidly with warming (e.g., O'Gorman & Muller, 2010). Because of these modifications to the atmospheric energy budget and physical state, various aspects of Earth's hydrologic cycle intensify (Dai, 2013; Donat et al., 2016; Fischer & Knutti, 2016; Giorgi et al., 2014; Held & Soden, 2006; Kharin et al., 2013; Min et al., 2011; Westra et al., 2013). A key measure of hydrologic cycle intensification is the change in global-mean precipitation. While it is clear that this quantity is projected to increase, there is a large spread in the magnitude of the increase (2–10% by 2100 under a high-emission scenario) among current global climate models (GCMs; Kharin et al., 2013). The spread partially arises due to different rates of surface warming (Fläschner et al., 2016; Kharin et al., 2013). Even after factoring in warming differences, a threefold spread in future precipitation change (1–3%/K) remains (Kharin et al., 2013).

Intermodel variability in global-mean precipitation change normalized by global-mean surface warming (ΔT), hereafter hydrologic sensitivity (HS), is a result of several factors, including differing *slow* and *fast* responses of

precipitation to increased atmospheric carbon dioxide (CO_2). The fast response is characterized by suppressed longwave radiative cooling and atmospheric warming due to the rapid adjustment of the land and atmosphere to increased CO_2, which increases atmospheric stability and reduces precipitation (Bony et al., 2013; Cao et al., 2012; Colman, 2015; DeAngelis et al., 2016; Richardson et al., 2016). The slow response is a result of the delayed oceanic warming that follows increased CO_2, which acts to increase precipitation in an attempt to offset increased net radiative cooling (Allen & Ingram, 2002; Andrews et al., 2010; Bala et al., 2010).

Recent work has evaluated the potential for the intermodel spread in HS to be constrained. There is a general consensus that the spread in the slow response is linked to structural differences in the parameterization of shortwave radiative transfer (DeAngelis et al., 2015; Fildier & Collins, 2015; Pendergrass & Hartmann, 2014a; Pincus et al., 2015). Furthermore, the change in global-mean precipitation is likely overestimated because of a common model bias related to this parameterization (DeAngelis et al., 2015). In comparison, model biases in HS due to the slow response of longwave cooling remain less definitive. While some studies suggest that longwave cooling (and thus HS) may be underestimated due to missing high-cloud processes (Mauritsen & Stevens, 2015; Su et al., 2017), a recent study suggests that longwave cooling may be overestimated due to low cloud biases (Watanabe et al., 2018). With regard to the fast precipitation response, previous work shows that intermodel differences in vegetation processes—specifically, the closure of leaf stomata—are strongly related to changes in turbulent heat fluxes, which in turn are closely linked to the fast component's intermodel spread (DeAngelis et al., 2016; Fläschner et al., 2016; Richardson et al., 2018). While a potentially important component of global HS, the fast response remains difficult to constrain because of limited observations related to vegetation processes. Despite this uncertainty, there is no strong indication of a model bias in either direction regarding the fast response (DeAngelis et al., 2016). In summary, the balance of previous work suggests that HS may be overestimated in GCMs, but additional modeling and observational studies are needed to strengthen this claim (e.g., Allan et al., 2014).

Another important aspect of hydrologic cycle intensification is changes in the temporal and spatial characteristics of precipitation, which have widespread implications for regional water security, natural hazard risks associated with droughts and floods, and ecosystem stability. For example, soils can absorb light-moderate rains effectively, but the same precipitation total over a shorter time period can cause flooding and runoff (Trenberth et al., 2003). Increasingly wide swings between extreme wet and extreme dry periods may also pose serious threats to both human infrastructure and natural systems adapted to historical precipitation regimes (e.g., Swain et al., 2018). Several studies have demonstrated the tendency for increased precipitation extremes (wet and dry) under a warming climate in both observations and models (Benestad, 2018; Giorgi et al., 2014; Gu & Adler, 2018; Lau et al., 2013; Lau & Wu, 2011; O'Gorman & Schneider, 2009; Trenberth et al., 2003). In addition, there is an established physical link between changes in extreme and nonextreme precipitation as increases in heavy rain events dry and stabilize the atmosphere, decreasing the frequency of light-moderate rainfall (Giorgi et al., 2011; Trenberth, 2009; Trenberth et al., 2003). This characteristic is generally captured by GCMs (Pall et al., 2007; Scoccimarro et al., 2013; Sun et al., 2007). For example, regions with projected increases in heavy precipitation also experience increases in the number of consecutive dry days (Lau et al., 2013; Sillmann et al., 2013). Like HS, the magnitude of changes in wet and dry extremes varies substantially across GCMs. It has been shown that most of the intermodel spread in wet extremes arises from tropical and subtropical regions (O'Gorman, 2012; O'Gorman & Schneider, 2009; Pendergrass & Hartmann, 2014b; Pfahl et al., 2017). Previous attempts to directly constrain projections in precipitation extremes are rather limited but have suggested that the increase in both wet and dry extremes, especially over land, may be underestimated by GCMs (Borodina et al., 2017; Douville & Plazzotta, 2017; O'Gorman, 2012).

One interesting question is whether constraints on global HS are relevant for the regional and temporal aspects of hydrologic cycle intensification that have more direct societal significance. For instance, is there a link in models between HS and projected changes in regional precipitation extremes? This question has been largely ignored in previous studies, and its answer can provide new insight on the practical value of reducing uncertainty in HS as well as offer a new perspective on the spread in extremes. In this paper, we investigate this topic in the current generation of GCMs, focusing on associations between the intermodel spread in HS and higher impact scales of projected precipitation change (including regional extremes). In the following section, specific methods are introduced. Results are given in section 3, and a discussion and conclusions are presented in section 4.

Table 1
List of Fifth Coupled Model Intercomparison Project (CMIP5) Models Analyzed, Their Institution, and Their Hydrologic Sensitivity (HS) Based on the RCP8.5 Emission Scenario

Model	Institution, country	HS (mm/day/K)
1. ACCESS1.0	Commonwealth Scientific and Industrial Research	0.049
2. ACCESS1.3	Organization and Bureau of Meteorology, Australia	0.056
3. BCC-CSM1.1	Beijing Climate Center, China Meteorological Administration, China	0.049
4. BCC-CSM1.1m		0.057
5. CanESM2	Canadian Centre for Climate Modelling and Analysis, Canada	0.040
6. CCSM4	National Center for Atmospheric Research, USA	0.050
7. CESM1-BGC	Community Earth System Model Contributors (NSF, DOE, NCAR), USA	0.050
8. CNRM-CM5	Centre National de Recherches Météorologiques, Centre Européen de Recherche et de Formation Avancée en Calcul Scientifique, France	0.049
9. CSIRO-Mk3.6.0	Commonwealth Scientific and Industrial Research Organization in collaboration with Queensland Climate Change Center of Excellence, Australia	0.053
10. GFDL-CM3	NOAA Geophysical Fluid Dynamics Laboratory, USA	0.051
11. GFDL-ESM 2G		0.034
12. GFDL-ESM 2M		0.031
13. HadGEM2-CC	Met Office Hadley Centre, UK	0.043
14. HadGEM2-ES		0.041
15. INM-CM4	Institute for Numerical Mathematics, Russia	0.043
16. IPSL-CM5A-LR	Institut Pierre-Simon Laplace, France	0.061
17. IPSL-CM5A-MR		0.061
18. IPSL-CM5B-LR		0.046
19. MIROC-ESM	Japan Agency for Marine-Earth Science and Technology, Atmosphere and	0.049
20. MIROC-ESM-CHEM	Ocean Research Institute (The University of Tokyo), and National	0.048
21. MIROC5	Institute for Environmental Studies, Japan	0.039
22. MPI-ESM-LR	Max Planck Institute for Meteorology, Germany	0.046
23. MPI-ESM-MR		0.050
24. MRI-CGCM3	Meteorological Research Institute, Japan	0.068
25. MRI-ESM 1		0.069
26. NorESM1-M	Norwegian Climate Centre, Norway	0.047

2. Data and Methods

We assess daily precipitation in 26 GCMs (Table 1) from the Fifth Coupled Model Intercomparison Project (CMIP5) using the historical and RCP8.5 (a high-emission scenario) experiments (Taylor et al., 2012). The future change in precipitation is defined as the difference between the 1960–1999 and 2060–2099 periods. All calculations are performed on each model's native grid, although we find that remapping to a common 2° by 2° grid leads to similar results (not shown). Additionally, only the first realization from each model is used to generate the CMIP5 ensemble statistics (mean, standard deviation, and correlation) discussed here.

A number of metrics to characterize the change in precipitation are computed throughout this paper, with slightly different approaches. For zonally resolved metrics, at each latitude, we first aggregate all days with precipitation above 0.1 mm across all longitudes (at the native model grid). Then we compute precipitation percentiles for both scenarios. The percent change in precipitation is calculated at every latitude and percentile for each model and divided by the future change in global-mean surface air (2 m) temperature (ΔT). We obtain similar results when using all days to compute the percentiles (not shown). Changes in precipitation are also calculated locally (grid cell scale). For this approach, we compute percentiles at each grid cell based on historical precipitation (again excluding values less than 0.1 mm/day). The percentile values are held fixed, then the total amount of precipitation falling within a range of percentiles or above/below a percentile (e.g., $\geq$99th) is calculated for both scenarios. The difference between RCP8.5 and the historical period can then be mapped or globally averaged. These differences are also divided by each model's global-mean 2 m temperature change to account for warming differences across the model ensemble. The method of holding percentile values fixed is also used in the calculation of future change histograms (hereafter difference histograms). The histogram bins are as follows: the first bin is from 0 to 0.1 mm/day, the second ranges from 0.1 mm/day to the 2.5th historical percentile, subsequent bins are in 2.5 percentile increments up to the 97.5th percentile, the next bin is the 97.5th to 99th percentile, and the last bin is equal to or greater than the 99th percentile (e.g., see Figure S1a).

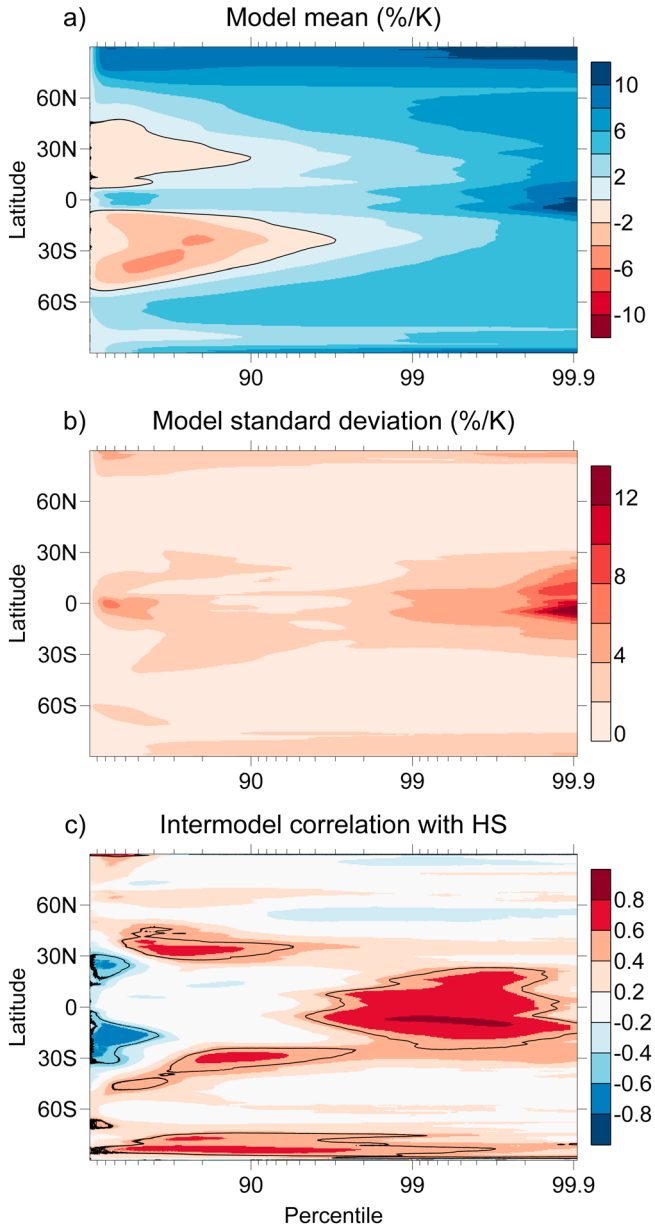

Figure 1. Projected change in precipitation as a function of latitude and percentile between 1960–1999 and 2060–2099. (a) The model-mean change, where the zero contour is shown in black. (b) The standard deviation of changes across models. (c) The intermodel correlation between the precipitation change at each latitude and percentile (mm/day/K) and hydrologic sensitivity (HS; mm/day/K). Correlations enclosed in the black contour are statistically significant, based on a two-tailed t test with $\alpha = 0.05$ and degrees of freedom corresponding to the number of subjectively determined independent models ($\nu = 15$). In all cases, the precipitation changes were normalized by each model's global-mean surface air temperature change prior to computing model statistics.

3. Results

3.1. Zonal Characteristics of Future Precipitation Change

The projected CMIP5 model-mean precipitation change with warming has distinct regional patterns when broken down zonally and by percentile. Figure 1a shows that precipitation at all percentiles is projected to increase across both equatorial (10°S–10°N) and high-latitude regions (poleward of 50°). On the other hand, the model-mean response in the areas within the subtropics to midlatitudes (10–45°) is characterized by a decrease in light-moderate rainfall and an increase in heavy-extreme precipitation (Figure 1a). Notably, this decrease in <90th percentile precipitation is much more pronounced in the Southern Hemisphere. The decrease in light-moderate precipitation in the subtropics to midlatitudes may be the energetic consequence of changes in the most extreme precipitation (>99th percentile), which increases across all latitudes, an argument set forward by Trenberth et al. (2003). The intensification of extreme precipitation events is strongest near the equator and over the high Arctic (~10%/K). This result largely agrees with the findings of Pall et al. (2007), who evaluated the zonal precipitation response from a single GCM (HadCM3). It should be noted that their reported values are much larger than what is shown here partly because we normalize the percent change in precipitation by warming. In addition, Pall et al. showed results from only one model, while we are computing an ensemble mean.

Figure 1b shows the intermodel spread in precipitation change as a function of latitude and percentile. The correlation between the zonal precipitation percentile changes and HS across models (Figure 1c) then reveals how this spread is connected to HS. We find that the increase in extreme events across the tropics (20°N–20°S) is significantly correlated ($r > 0.6$) with HS. That is, models with a larger global-mean precipitation change also feature a stronger intensification of tropical precipitation extremes. Additionally, there are significant subtropical signals at somewhat lower percentiles in both hemispheres, which appear to be associated with regional atmospheric river corridors (see section 3.2). Together, this evidence suggests that increases in tropical extremes and atmospheric river events may account for much of the required latent heat increase when the global hydrologic cycle intensifies. Therefore, the future increase in tropical and some extratropical extremes (e.g., atmospheric rivers) is closely linked to the global-mean hydrologic cycle change.

3.2. Local Features of Future Precipitation Change

To better understand the relationship between HS and local precipitation changes, we investigate the intermodel correlations for a series of measures at the grid cell scale. First, we compare the change in local total precipitation ($\Delta P/\Delta T$) with HS (Figure 2a) to highlight regions where local precipitation change scales with the globally-averaged change. (See Figure S2 for the spatial patterns of climatological precipitation and its projected changes in the CMIP5 ensemble.) Although no coherent pattern emerges on large scales, there is a significant positive correlation across the atmospheric river prone regions of the Northern Hemisphere (e.g., portions of the North Pacific and North Atlantic), indicating that models with strong HS also have large local changes in total precipitation over these regions. On the other hand, there are a few climatologically dry subtropical oceanic regions (over the Atlantic near West Africa and over the eastern South Pacific and the western South Atlantic on either side of South America) where the correlation is significantly negative. The zonal asymmetry of the subtropical

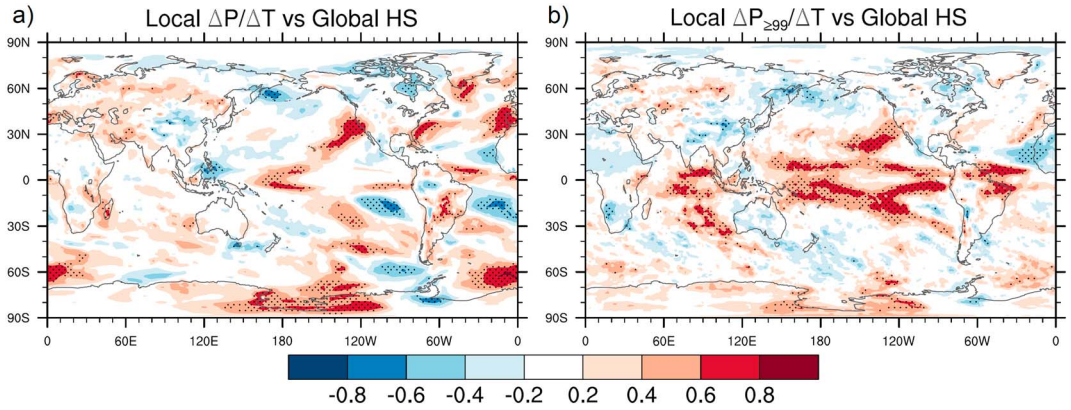

Figure 2. Intermodel correlation between global hydrologic sensitivity (HS) and (a) local $\Delta P/\Delta T$ or (b) the local change in extreme (≥99th percentile) precipitation per degree of global-mean warming ($\Delta P_{\geq 99}/\Delta T$). Statistically significant correlations are stippled.

precipitation response (Figure 2a) may help to reconcile the apparent conflict between studies on its global uniformity (Greve et al., 2014; He & Soden, 2016). That is, the subtropical/lower midlatitude locations where atmospheric rivers are prevalent may experience a response more consistent with the wetting tropics, whereas the rest of the subtropics are largely dominated by the *dry get drier* effect (Figure 2a).

Next, we look at the correlation between the change in local extreme precipitation (≥99th percentile; $\Delta P_{\geq 99}/\Delta T$) and HS (Figure 2b). As expected from Figure 1c, the future intensification of extreme precipitation in much of the tropics is significantly correlated ($r > 0.6$) with HS across models. These significant correlations occur mostly over oceanic regions but also extend to parts of South America. Compared to the case of total precipitation (Figure 2a), significant positive correlations are far more extensive between HS and extreme precipitation in the tropics. In both cases significant correlations are detected in extratropical regions that favor the development of atmospheric rivers (e.g., the northeastern Pacific Ocean west of North America). This is particularly noteworthy in light of the fact that transient atmospheric rivers are collectively responsible for over 90% of poleward water vapor flux at the latitudes where they are found (Zhu & Newell, 1998) and consequently a substantial fraction of moist static energy transport (Hwang & Frierson, 2010).

These results suggest that the considerable spread in projected changes in tropical and in certain cases extratropical precipitation extremes may be reduced through efforts to reduce spread in HS and the global atmospheric energy budget. An assessment of the relationship between extreme precipitation and the atmospheric energy budget shows that changes in all components (i.e., longwave cooling, shortwave absorption, and sensible heat) are associated with the corresponding increase in precipitation extremes (Figure S3).

3.3. Compensation Across the Precipitation Distribution

The precipitation distribution changes are shaped not only by HS but also by dynamics within a particular model, especially compensation between changes in extreme and nonextreme portions of the distribution. To demonstrate this effect, for each CMIP5 model, we compute the fraction of globally averaged precipitation change arising from extreme (≥99th percentile) and nonextreme (<99th percentile) events (global-mean $\Delta P_{\geq 99}/\Delta T$ and $\Delta P_{<99}/\Delta T$, respectively) and scatter these two quantities (Figure 3a). We find them to be very strongly anticorrelated across the CMIP5 ensemble ($r = -0.83$). This result is highly robust across three key choices relating to definitions of *extreme* and *nonextreme* precipitation: (1) the percentile used to differentiate extreme and nonextreme precipitation (e.g., 90th, 95th, and 99th), (2) whether or not dry days (e.g., <20th percentile) are included in the definition of nonextreme precipitation, and (3) whether we consider only those locations with *increasing* extreme precipitation and *decreasing* nonextreme precipitation when computing the global mean or all areas (not shown). The anticorrelation between extreme and nonextreme parts of the distribution is also found when difference histograms are first globally averaged (Figure S1b). These findings demonstrate that if a model exhibits larger increases in precipitation during heavy events, it will have generally larger decreases (or smaller increases) during light-moderate events. From a physical point of view, this result supports earlier findings (Giorgi et al., 2011; Rasmussen et al., 2017; Trenberth, 2009; Trenberth

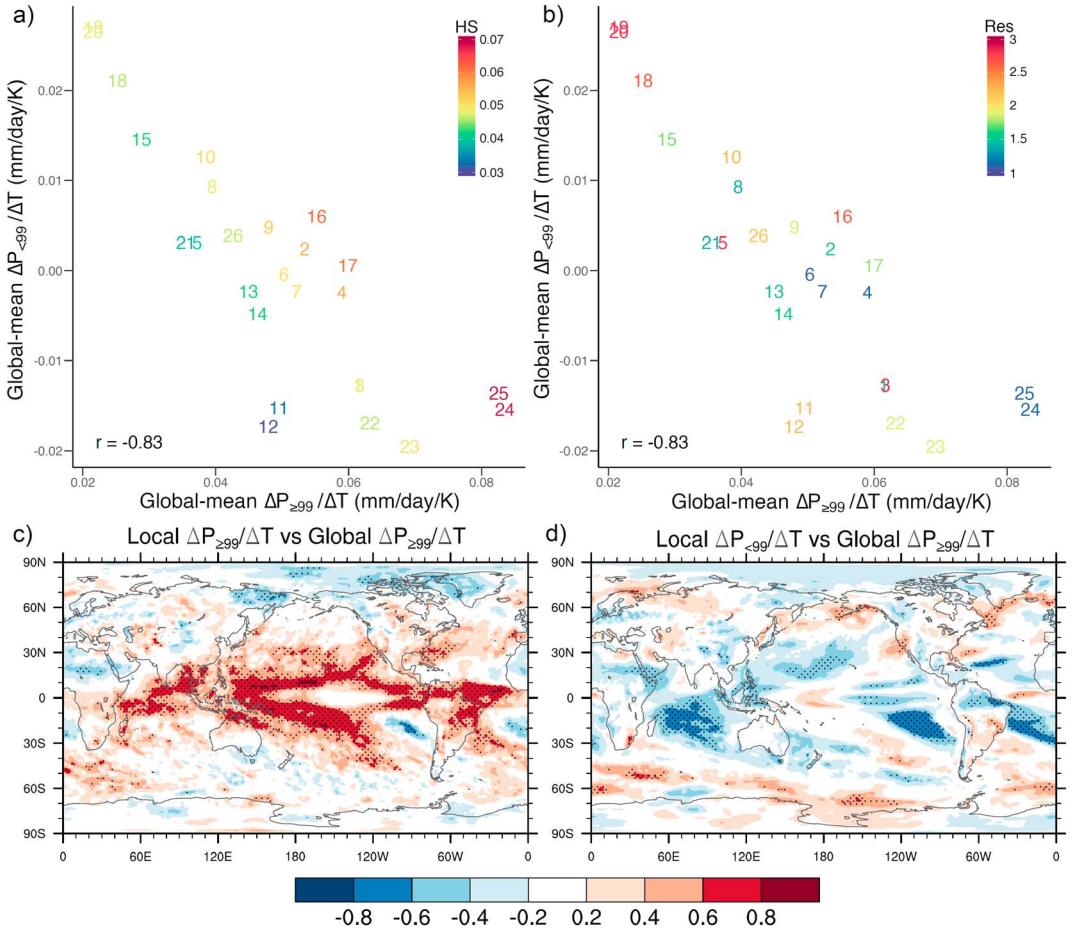

Figure 3. Intermodel relationship between projected changes in extreme and nonextreme precipitation. Top: Scatterplots of global-mean $\Delta P_{\geq 99}/\Delta T$ versus global-mean $\Delta P_{<99}/\Delta T$. Each model is numbered according to Table 1 and color-coded by (a) its hydrologic sensitivity (HS; mm/day/K) and (b) its resolution. The resolution is expressed as the length of the side of an atmospheric grid cell (in degrees) if the grid cell was a square. Bottom: The intermodel correlation between global-mean $\Delta P_{\geq 99}/\Delta T$ and (c) local $\Delta P_{\geq 99}/\Delta T$ or (d) local $\Delta P_{<99}/\Delta T$. Statistically significant correlations are stippled.

et al., 2003): Through larger latent heat release, intense downpours may stabilize the atmosphere more when the increase in extremes is larger. This effect leads to larger and possibly more spatially extensive suppression in less intense events, an effect we confirm below. Our new results thus demonstrate that the established relationship between changes in extreme and nonextreme precipitation found within individual models and observations (e.g., Giorgi et al., 2014) also applies within the context of intermodel spread.

We examine the regions contributing to the anticorrelation in Figure 3a by computing the intermodel correlation between global-mean $\Delta P_{\geq 99}/\Delta T$ and local $\Delta P_{\geq 99}/\Delta T$ (Figure 3c) and between global-mean $\Delta P_{\geq 99}/\Delta T$ and local $\Delta P_{<99}/\Delta T$ (Figure 3d). These figures show that GCMs with a stronger increase in tropical extremes (i.e., having a larger global-mean $\Delta P_{\geq 99}/\Delta T$; Figure 3c) tend to exhibit a larger decrease (or smaller increase) in subtropical light-moderate precipitation events (Figure 3d). Thus, while a local trade-off between changes in extreme and nonextreme precipitation appears to occur in some places (e.g., the northern Indian and Pacific Oceans), the trade-off is primarily nonlocal in nature (Figures 3c and 3d). Nonlocal compensation implies that drying and stabilizing of the atmosphere caused by increasing wet extremes tend to suppress the frequency of lighter events in adjacent, drier subtropical regions.

Figures 3a and 3b also offer an overview of factors shaping simulated future changes in the precipitation distribution. Consistent with the results in sections 3.1 and 3.2, global-mean $\Delta P_{\geq 99}/\Delta T$ is significantly correlated with global HS ($r = 0.58$; see also the color coding in Figure 3a). Thus, one factor behind the model differences in Figure 3 (in particular, the spread in wet extremes) is the degree to which global-mean

precipitation intensifies. Further insight is gained by investigating the influence of atmospheric model resolution on the projected changes. Prior work has suggested that higher resolution models better capture extreme precipitation (Kopparla et al., 2013) because coarser models must rely more heavily on parameterizations to handle physical processes related to rising motion and convection (Shiu et al., 2012). We find that the change in global-mean $\Delta P_{\geq 99}/\Delta T$ tends to be weaker in models with coarser resolution than those with finer resolution ($r = -0.50$, see colors in Figure 3b). However, in the case of the CMIP5 ensemble, even the finest resolution models (~100 km) still must rely heavily on parameterized updraft and convection in many regions, likely limiting the strength of this relationship. Resolution is just one potential source of model spread, and further work is needed to better understand additional physical and parametric sources for the model spread in changes in precipitation extremes. We note that in Figure 3a, the models are striated diagonally by color, with the models with the highest HS located toward the upper right, and lowest HS toward the lower left. (This behavior is consistent with the fact that the sum of the *x* and *y* axis values equals HS.) For models with the same HS, it seems likely that dynamics, themselves heavily influenced by resolution, shape the change in the most extreme events. The nonextreme events must then adjust to be consistent with the model's HS.

4. Discussion and Conclusions

In this study, we find that the future intensification of extreme precipitation in the tropics and in subtropical atmospheric river corridors is significantly correlated with the global-mean total precipitation change per degree warming across the CMIP5 ensemble. This implies that increases in tropical extremes and large atmospheric river events account for much of the required latent heat increase when the global hydrologic cycle intensifies. In other words, the degree to which the global hydrologic cycle intensifies matters for the increase in extreme precipitation in much of the world. An implication is that constraining the global precipitation increase, through consideration of the atmospheric energy budget, could help reduce the intermodel spread in projections of extreme precipitation. The task of constraining HS in models is therefore more than merely an academic exercise, as it may shed light on other aspects of hydrologic cycle intensification with greater practical relevance. We also show that increasing model resolution may lead to larger increases in global wet extremes, which originate predominantly in the tropics. Our results offer new perspectives on the intermodel spread in extreme precipitation change, particularly in the tropics. The results complement previous studies, which have highlighted interannual variability, atmospheric dynamics, and convective parameterizations with regard to understanding and constraining the spread in tropical extremes (O'Gorman, 2012; O'Gorman & Schneider, 2009; Pfahl et al., 2017).

Another finding shown here is that changes in extreme precipitation are highly anticorrelated with changes in light-moderate precipitation across models. This represents another strong constraint on hydrologic cycle change: In the absence of any change in the overall energy budget, changes in one part of the distribution have to be compensated by changes in the rest of the distribution. This robust linkage suggests that constraints placed on tropical extremes would translate into constraints on the projected change in light-moderate precipitation. We present evidence that this trade-off may occur in a spatially inhomogeneous sense—with large increases in tropical (and, locally, midlatitude atmospheric river) precipitation extremes occurring at the expense of more moderate precipitation events elsewhere in the subtropics and lower midlatitudes.

Signs of the trade-off between precipitation extremes and the rest of the distribution are being detected in the observational record (Gu & Adler, 2018). Such observational measurements may offer additional insight and guidance for the task of constraining model uncertainty surrounding future extreme precipitation. Future studies could also explore further the physical mechanisms linking extreme precipitation and the atmospheric energy budget components (Figure S3). Controlled simulations with individual GCMs could be particularly useful with this task. Additionally, the degree to which projections of global precipitation change are biased, especially with regard to changes in longwave cooling (Mauritsen & Stevens, 2015; Su et al., 2017; Watanabe et al., 2018), requires more investigation. In short, our results offer directions for future research to complement and expand on the currently limited body of work on constraining uncertainty surrounding future changes in the precipitation distribution, especially wet extremes.

Acknowledgments
We acknowledge funding from the National Science Foundation grant (1543268) titled "Reducing Uncertainty Surrounding Climate Change Using Emergent Constraints," and the Regional and Global Climate Program for the Office of Science of the U.S. DOE. D. L. S. was supported by a Nature Conservancy NatureNet Fellowship and the UCLA Sustainable LA Grand Challenge. We thank two anonymous reviewers for their helpful comments. We also thank the World Climate Research Programme's Working Group on Coupled Modeling and the individual modeling groups for making CMIP5 data available (https://esgf-node.llnl.gov/projects/esgf-llnl/).

References

Allan, R. P., Liu, C., Zahn, M., Lavers, D. A., Koukouvagias, E., & Bodas-Salcedo, A. (2014). Physically consistent responses of the global atmospheric hydrological cycle in models and observations. *Surveys in Geophysics*, *35*(3), 533–552. https://doi.org/10.1007/s10712-012-9213-z

Allen, M. R., & Ingram, W. J. (2002). Constraints on future changes in climate and the hydrologic cycle. *Nature*, *419*(6903), 224–232. https://doi.org/10.1038/nature01092

Andrews, T., Forster, P. M., Boucher, O., Bellouin, N., & Jones, A. (2010). Precipitation, radiative forcing and global temperature change. *Geophysical Research Letters*, *37*, L14701. https://doi.org/10.1029/2010GL043991

Bala, G., Caldeira, K., & Nemani, R. (2010). Fast versus slow response in climate change: Implications for the global hydrological cycle. *Climate Dynamics*, *35*(2-3), 423–434. https://doi.org/10.1007/s00382-009-0583-y

Benestad, R. (2018). Implications of a decrease in the precipitation area for the past and the future. *Environmental Research Letters*, *13*(4), 044022.https://doi.org/10.1088/1748-9326/aab375.

Bony, S., Bellon, G., Klocke, D., Sherwood, S., Fermepin, S., & Denvil, S. (2013). Robust direct effect of carbon dioxide on tropical circulation and regional precipitation. *Nature Geoscience*, *6*(6), 447–451. https://doi.org/10.1038/ngeo1799

Borodina, A., Fischer, E. M., & Knutti, R. (2017). Models are likely to underestimate increase in heavy rainfall in the extratropical regions with high rainfall intensity. *Geophysical Research Letters*, *44*, 7401–7409. https://doi.org/10.1002/2017GL074530

Cao, L., Bala, G., & Caldeira, K. (2012). Climate response to changes in atmospheric carbon dioxide and solar irradiance on the time scale of days to weeks. *Environmental Research Letters*, *7*(3), 1–8. https://doi.org/10.1088/1748-9326/7/3/034015

Colman, R. A. (2015). Climate radiative feedbacks and adjustments at the Earth's surface. *Journal of Geophysical Research: Atmospheres*, *120*, 3173–3182. https://doi.org/10.1002/2014JD022896

Dai, A. (2013). Increasing drought under global warming in observations and models. *Nature Climate Change*, *3*(1), 52–58. https://doi.org/10.1038/nclimate1633

DeAngelis, A. M., Qu, X., & Hall, A. (2016). Importance of vegetation processes for model spread in the fast precipitation response to CO2 forcing. *Geophysical Research Letters*, *43*, 12,550–12,559. https://doi.org/10.1002/2016GL071392

DeAngelis, A. M., Qu, X., Zelinka, M. D., & Hall, A. (2015). An observational radiative constraint on hydrologic cycle intensification. *Nature*, *528*(7581), 249–253. https://doi.org/10.1038/nature15770

Donat, M. G., Lowry, A. L., Alexander, L. V., O'Gorman, P. A., & Maher, N. (2016). More extreme precipitation in the world's dry and wet regions. *Nature Climate Change*, *6*, 508–513. https://doi.org/10.1038/nclimate3160

Douville, H., & Plazzotta, M. (2017). Midlatitude summer drying: An underestimated threat in CMIP5 models? *Geophysical Research Letters*, *44*, 9967–9975. https://doi.org/10.1002/2017GL075353

Fildier, B., & Collins, W. D. (2015). Origins of climate model discrepancies in atmospheric shortwave absorption and global precipitation changes. *Geophysical Research Letters*, *42*, 8749–8757. https://doi.org/10.1002/2015GL065931

Fischer, E. M., & Knutti, R. (2016). Observed heavy precipitation increase confirms theory and early models. *Nature Climate Change*, *6*(11), 986–991. https://doi.org/10.1038/nclimate3110

Fläschner, D., Mauritsen, T., & Stevens, B. (2016). Understanding the intermodel spread in global-mean hydrological sensitivity*. *Journal of Climate*, *29*(2), 801–817. https://doi.org/10.1175/JCLI-D-15-0351.1

Giorgi, F., Coppola, E., & Raffaele, F. (2014). A consistent picture of the hydroclimatic response to global warming from multiple indices: Models and observations. *Journal of Geophysical Research: Atmospheres*, *119*, 11,695–11,708. https://doi.org/10.1002/2014JD022238

Giorgi, F., Im, E. S., Coppola, E., Diffenbaugh, N. S., Gao, X. J., Mariotti, L., & et al. (2011). Higher hydroclimatic intensity with global warming. *Journal of Climate*, *24*(20), 5309–5324. https://doi.org/10.1175/2011JCLI3979.1

Greve, P., Orlowsky, B., Mueller, B., Sheffield, J., Reichstein, M., & Seneviratne, S. I. (2014). Global assessment of trends in wetting and drying over land. *Nature Geoscience*, *7*(10), 716–721. https://doi.org/10.1038/NGEO2247

Gu, G., & Adler, R. F. (2018). Precipitation intensity changes in the tropics from observations and models. *Journal of Climate*, *31*(12), 4775–4790.https://doi.org/10.1175/JCLI-D-17-0550.1.

He, J., & Soden, B. J. (2016). A re-examination of the projected subtropical precipitation decline. *Nature Climate Change*, *7*(1), 53–57. https://doi.org/10.1038/nclimate3157

Held, I. M., & Soden, B. J. (2006). Robust responses of the hydrological cycle to global warming. *Journal of Climate*, *19*(21), 5686–5699. https://doi.org/10.1175/JCLI3990.1.

Hwang, Y. T., & Frierson, D. M. W. (2010). Increasing atmospheric poleward energy transport with global warming. *Geophysical Research Letters*, *37*, L24807. https://doi.org/10.1029/2010GL045440

Kharin, V. V., Zwiers, F. W., Zhang, X., & Wehner, M. (2013). Changes in temperature and precipitation extremes in the CMIP5 ensemble. *Climatic Change*, *119*(2), 345–357. https://doi.org/10.1007/s10584-013-0705-8

Kopparla, P., Fischer, E. M., Hannay, C., & Knutti, R. (2013). Improved simulation of extreme precipitation in a high-resolution atmosphere model. *Geophysical Research Letters*, *40*, 5803–5808. https://doi.org/10.1002/2013GL057866

Lau, W. K.-M., Wu, H., & Kim, K. (2013). A canonical response of precipitation characteristics to global warming from CMIP5 models. *Geophysical Research Letters*, *40*, 3163–3169. https://doi.org/10.1002/grl.50420

Lau, W. K.-M., & Wu, H. T. (2011). Climatology and changes in tropical oceanic rainfall characteristics inferred from Tropical Rainfall Measuring Mission (TRMM) data (1998 – 2009). *Journal of Geophysical Research*, *116*, D17111. https://doi.org/10.1029/2011JD015827

Mauritsen, T., & Stevens, B. (2015). Missing iris effect as a possible cause of muted hydrological change and high climate sensitivity in models. *Nature Geoscience*, *8*(5), 346–351. https://doi.org/10.1038/NGEO2414

Min, S. K., Zhang, X., Zwiers, F. W., & Hegerl, G. C. (2011). Human contribution to more-intense precipitation extremes. *Nature*, *470*(7334), 378–381. https://doi.org/10.1038/nature09763

O'Gorman, P. A. (2012). Sensitivity of tropical precipitation extremes to climate change. *Nature Geoscience*, *5*(10), 697–700. https://doi.org/10.1038/ngeo1568

O'Gorman, P. A., & Muller, C. J. (2010). How closely do changes in surface and column water vapor follow Clausius-Clapeyron scaling in climate change simulations? *Environmental Research Letters*, *5*(2), 025207. https://doi.org/10.1088/1748-9326/5/2/025207

O'Gorman, P. A., & Schneider, T. (2009). The physical basis for increases in precipitation extremes in simulations of 21st-century climate change. *Proceedings of the National Academy of Sciences*, *106*(35), 14,773–14,777. https://doi.org/10.1073/pnas.0907610106

Pall, P., Allen, M. R., & Stone, D. A. (2007). Testing the Clausius-Clapeyron constraint on changes in extreme precipitation under CO_2 warming. *Climate Dynamics*, *28*(4), 351–363. https://doi.org/10.1007/s00382-006-0180-2

Pendergrass, A. G., & Hartmann, D. L. (2014a). The atmospheric energy constraint on global-mean precipitation change. *Journal of Climate*, *27*(2), 757–768. https://doi.org/10.1175/JCLI-D-13-00163.1

Pendergrass, A. G., & Hartmann, D. L. (2014b). Changes in the distribution of rain frequency and intensity in response to global warming. *Journal of Climate*, *27*(22), 8372–8383. https://doi.org/10.1175/JCLI-D-14-00183.1

Pfahl, S., O'Gorman, P. A., & Fischer, E. M. (2017). Understanding the regional pattern of projected future changes in extreme precipitation. *Nature Climate Change*, *7*(6), 423–427. https://doi.org/10.1038/nclimate3287

Pincus, R., Mlawer, E. J., Oreopoulos, L., Ackerman, A. S., Baek, S., Brath, M., et al. (2015). Radiative flux and forcing parameterization error in aerosol-free clear skies. *Geophysical Research Letters*, *42*, 5485–5492. https://doi.org/10.1002/2015GL064291

Rasmussen, K. L., Prein, A. F., Rasmussen, R. M., Ikeda, K., & Liu, C. (2017). Changes in the convective population and thermodynamic environments in convection-permitting regional climate simulations over the United States. *Climate Dynamics*, 1–26. https://doi.org/10.1007/s00382-017-4000-7

Richardson, T. B., Forster, P. M., Andrews, T., Boucher, O., Faluvegi, G., Fläschner, D., et al. (2018). Carbon dioxide physiological forcing dominates projected eastern Amazonian drying. *Geophysical Research Letters*, *45*, 2815–2825. https://doi.org/10.1002/2017GL076520

Richardson, T. B., Samset, B. H., Andrews, T., Myhre, G., & Forster, P. M. (2016). An assessment of precipitation adjustment and feedback computation methods. *Journal of Geophysical Research: Atmospheres*, *121*, 11,608–11,619. https://doi.org/10.1002/2016JD025625

Scoccimarro, E., Gualdi, S., Bellucci, A., Zampieri, M., & Navarra, A. (2013). Heavy precipitation events in a warmer climate: Results from CMIP5 models. *Journal of Climate*, *26*(20), 7902–7911. https://doi.org/10.1175/JCLI-D-12-00850.1

Shiu, C. J., Liu, S. C., Fu, C., Dai, A., & Sun, Y. (2012). How much do precipitation extremes change in a warming climate? *Geophysical Research Letters*, *39*, L17707. https://doi.org/10.1029/2012GL052762

Sillmann, J., Kharin, V. V., Zwiers, F. W., Zhang, X., & Bronaugh, D. (2013). Climate extremes indices in the CMIP5 multimodel ensemble: Part 2. Future climate projections. *Journal of Geophysical Research: Atmospheres*, *118*, 2473–2493. https://doi.org/10.1002/jgrd.50188

Su, H., Jiang, J. H., Neelin, J. D., Shen, T. J., Zhai, C., Yue, Q., et al. (2017). Tightening of tropical ascent and high clouds key to precipitation change in a warmer climate. *Nature Communications*, *8*, 1–9. https://doi.org/10.1038/ncomms15771

Sun, Y., Solomon, S., Dai, A., & Portmann, R. W. (2007). How often will it rain? *Journal of Climate*, *20*(19), 4801–4818. https://doi.org/10.1175/JCLI4263.1

Swain, D. L., Langenbrunner, B., Neelin, J. D., & Hall, A. (2018). Increasing precipitation volatility in 21st century California. *Nature Climate Change*, *8*(5), 427–433. https://doi.org/10.1038/s41558-018-0140-y

Taylor, K. E., Stouffer, R. J., & Meehl, G. a. (2012). An overview of CMIP5 and the experiment design. *Bulletin of the American Meteorological Society*, *93*(4), 485–498. https://doi.org/10.1175/BAMS-D-11-00094.1

Trenberth, K. E. (2009). Precipitation in a changing climate—More floods and droughts in the future. *GEWEX News*, *19*(May 2009), 8–10.

Trenberth, K. E., Dai, A., Rasmussen, R. M., & Parsons, D. B. (2003). The changing character of precipitation. *Bulletin of the American Meteorological Society*, 1205–1217. https://doi.org/10.1175/BAMS-84-9-1205

Watanabe, M., Kamae, Y., Shiogama, H., DeAngelis, A. M., & Suzuki, K. (2018). Low clouds link equilibrium climate sensitivity to hydrological sensitivity. *Nature Climate Change*, *8*(10), 901–906. https://doi.org/10.1038/s41558-018-0272-0

Westra, S., Alexander, L. V., & Zwiers, F. W. (2013). Global increasing trends in annual maximum daily precipitation. *Journal of Climate*, *26*(11), 3904–3918. https://doi.org/10.1175/JCLI-D-12-00502.1

Zhu, Y., & Newell, R. E. (1998). A proposed algorithm for moisture fluxes from atmospheric rivers. *Monthly Weather Review*, *126*(3), 725–735. https://doi.org/10.1175/1520-0493(1998)126<0725:APAFMF>2.0.CO;2